June 1998 DESY PRC 98/06

Proposal for an Upgrade of the H1 Forward Track Detector for HERA 2000

H1 Collaboration

Abstract

It is planned to increase the luminosity delivered by the HERA ep collider by a factor of about 5 in the year 2000, making it possible to study in detail the highest energy electron-quark collisions yet achieved and opening a discovery window for new physics. These collisions occur in the high Bjorken-x, high Q^2 region of the deep-inelastic scattering kinematic plane and result in both the scattered electron and the produced hadrons travelling in the proton (*i.e.* forward) direction in the H1 detector. In order to increase the efficiency and precision with which H1 can study these interactions, it is proposed to upgrade the Forward Track Detector (FTD). The upgrade will reduce both the statistical and systematic errors associated with measurements made using the FTD, increase its discovery potential and allow a variety of novel QCD effects to be studied.

1 Introduction

The HERA accelerator at DESY in Hamburg currently collides 820 GeV protons with 27.5 GeV positrons. The highest annual integrated luminosity achieved to date is $34.6\,\mathrm{pb}^{-1}$ in 1997. Modifications to HERA, to be carried out in the year 2000, will increase the luminosity delivered to about $150\,\mathrm{pb}^{-1}$ per year [1]. This will enable the HERA experiments to study in detail the largely unexplored high Q^2 and large x region in deep-inelastic scattering (DIS). This kinematic domain gives the largest possible electron-quark centre-of-mass energy and is thus the region in which any new phenomena are most likely to be discovered. Interactions in the high x and high Q^2 region result in the scattered lepton and the produced hadrons travelling in the proton (forward) direction. It will therefore be important to have the best possible measurement of charged particle tracks in the forward region of the HERA detectors to enable detailed study of any new phenomena which occur.

In the H1 detector, charged particle measurements in the forward region are made using the Forward Track Detector (FTD). The current apparatus has a hadronic track finding efficiency for well measured tracks of below 50% in events with high forward multiplicity, rising to 90% for the simplest events, such as elastic J/ψ production. As is discussed in more detail in the following, the poor efficiency at high multiplicities is caused by the large number of hodoscope ambiguities in such events, a problem aggravated by secondary interactions in parts of the detector and the beam pipe and associated collimators. The number of such secondary interactions is likely to be somewhat larger following the HERA upgrade.

The goal of the proposal made in this document is to increase the efficiency of the FTD to above 90% in high multiplicity events. This is to be achieved by inserting extra chambers into the FTD, adding redundancy and hence allowing tracks to be extracted from the complex environment arising due to the high primary and secondary track density mentioned above. Specifically, we propose to replace the MWPCs and the transition radiators, which will not be used in future operations, by three extra planar chambers.

The improvements described will ensure that H1 is in the best possible position to search for new phenomena in the kinematic region to be explored in detail when the high luminosity becomes available. In addition, it will make possible some studies of novel QCD processes and also improve significantly the precision with which others can be measured. In the following, some of the measurements which would benefit from the proposed improvements to the FTD are described, as are the means of achieving those improvements. If approved, the modifications proposed here would be made in parallel with the upgrade of the HERA collider.

2 Physics with the FTD

2.1 Introduction

To date, the FTD has been used to determine the position of the z vertex [2, 3] in DIS events and as a veto in various studies of the production of heavy quarks [4]. It has also been used to study charged particle transverse momentum spectra in both DIS [5] and photoproduction events [6], and has made a contribution to measurements of fragmentation and multiplicity distributions in the current hemisphere of the Breit frame [7]. These last three studies required high quality, well measured tracks, detected in the current FTD with an efficiency of about 50%. Large correction factors must thus be applied and the multiplicity dependence of the efficiency ensures that these correction factors are model dependent, giving rise to significant systematic errors. During high luminosity running, measurements of any new phenomena which appear will suffer from similar problems if the FTD is not improved.

2.2 The high Q^2, high x region

The primary goal of the HERA upgrade is to search for evidence of new physics in DIS at the highest possible Q^2 values. In 1997 both HERA experiments saw tantalising hints that new physics may be on the horizon [8, 9]; more events were observed than predicted by Standard Model (SM) calculations at the highest values of Q^2 currently accessible. Regardless of whether these hints are eventually confirmed or turn out to be statistical fluctuations, it is clear that the forward region will be particularly important in searches for new physics and that these would benefit from improvements to the FTD. By virtue of the asymmetric beam energies, any new high mass state produced at HERA will travel in the proton direction and its decay products will be seen largely in the forward region. As an example, either the electron or the quark jet resulting from the decay of a scalar leptoquark of mass $200\,\mathrm{GeV/c^2}$ is found within the FTD 75% of the time. This proportion increases to 100% for a leptoquark mass of $250\,\mathrm{GeV/c^2}$.

2.3 QCD studies

2.3.1 Introduction

In addition to the improved discovery potential arising from the FTD upgrade, a programme of novel rarer QCD effects can be studied. Much remains to be done to improve our understanding of the SM in this respect. Detailed studies of the parton densities within the proton, particularly the relatively poorly measured gluon density, and their evolution with Q^2 provide an important test of QCD, as well as being essential input for calculations relevant to future experiments. The significance of the forward region is illustrated here with reference to the study of charm in ep interactions.

2.3.2 Heavy quark production

Much work has already been done on the production of charm in DIS at small x at HERA [10, 11]. The FTD upgrade will enable us to extend these studies to high values of x. This allows comparison with the fixed target data [12], and the extension of these measurements to higher Q^2 values. Charm has been shown to be produced mainly by the boson gluon fusion (BGF) mechanism [10] and hence such studies will be sensitive to any anomalous high x gluon content of the proton. In addition, charm production at high x will be sensitive to the presence of charm quark Fock states in the proton, such as intrinsic charm [13].

The presence of charm may be detected by identifying $D^{\star+}$ mesons[1] via their decay $D^{\star+} \to D^0\pi^+$ and the subsequent decay $D^0 \to K^-\pi^+$. The difference between the masses of the $D^\star$ and D^0 mesons is small and thus the quantity $m_{D^\star} - m_{D^0}$ can be determined precisely and the decay chain easily identified as the phase space production of $K^-\pi^+\pi^+$ systems with this mass difference is strongly suppressed. The observation of this $D^\star$ decay mode requires the detection of the three charged decay products in a high multiplicity environment. Currently, such measurements in the FTD are seriously hampered by the attainable tracking efficiency. If some or all of the decay products are within the geometrical acceptance of the FTD, the upgrade proposed here results in a large increase in the efficiency for identifying $D^\star$ mesons.

In order to quantify the expected gains due to the proposed FTD upgrade, a Monte Carlo study was made of the charm identification efficiency attainable in DIS in the forward region using the current and upgraded Forward Track Detectors. Events were generated using the LEPTO 6.5 [14] Monte Carlo program and passed through a simulation of the current H1

[1] Throughout this section, charge conjugate states are always implicitly included.

detector. Events in which the activity was largely in the forward direction were then selected, assuming the process involved was the scattering of a quark with four-momentum xp out of the proton by a photon with four-momentum q. The four-momentum of the struck quark, k, is then $k = q + xp$, from which its polar angle, θ_q, can be determined. It was required that $\theta_q < 30^\circ$, $Q^2 > 4\,\mathrm{GeV}^2$ and $x > 0.007$.

Using the sub-sample of forward events, a search was made for $D^\star$ decays using all charged tracks in the central track detector (CTD) and the FTD. The track parameters were smeared in accordance with the resolutions currently obtained in the CTD and the FTD, and realistic tracking efficiencies were assumed for both detectors. All pairs of detected charged particles with transverse momenta greater than $0.4\,\mathrm{GeV/c}$ were considered as candidate $D^0 \to K^-\pi^+$ decay products. At least one of the pair was required to be within the FTD acceptance. The particles were assumed to be K and π mesons, both possible K and π combinations being tried. The mass of the pair's summed four-momentum, $m_{K\pi}$, was formed, and combinations with $|m_{K\pi} - m_{D^0}| < 100\,\mathrm{MeV/c^2}$, where m_D^0 is the nominal D^0 mass, were considered to arise from D^0 decays. A histogram of the $m_{K\pi}$ mass values obtained is shown in figure 1a. A search was made for a further particle with transverse momentum greater than $150\,\mathrm{MeV/c}$ and charge opposite to that of the kaon. If such a particle was found, this was assumed to be the "slow pion" in the $D^{\star+} \to D^0\pi^+$ decay and the candidate $D^\star$ meson mass, $m_{K\pi\pi}$, was formed. The transverse momentum of the $D^\star$ candidates was required to be greater than $2\,\mathrm{GeV/c}$ and their polar angle to be in the range $10^\circ < \theta < 20^\circ$. The mass difference $\Delta m = |m_{K\pi\pi} - m_{K\pi}|$ was then entered in a histogram. The background contribution to this histogram was taken to be given by the Δm distribution obtained using the wrong sign combinations, *i.e.* in which the slow pion has the same charge as the kaon, and was subtracted. The resulting Δm distribution is shown in figure 1b.

The above procedure was repeated using Monte-Carlo data in which the performance of the upgraded FTD was simulated, making the conservative assumption that the amount of material and hence that the multiple coulomb scattering and the attainable momentum resolution in the new FTD are the same as in the current system, but that the hadron detection efficiency is improved as described below. As can be seen in figure 1b, using the upgraded FTD gives rise to a clear peak in the Δm distribution at the value expected from the decay $D^\star \to D^0\pi$, whereas using the current FTD this peak is much less significant. The above selection procedure gives an expected number of 900 $D^\star$ mesons per $150\,\mathrm{pb}^{-1}$ year detected in the forward region if the upgraded FTD is used. The current system allows approximately 200 of these to be found.

The proposed upgrade would thus have a large impact, allowing charm to be identified down to polar angles of about 10°. Current H1 studies in DIS [10] are limited to $\theta \gtrsim 25^\circ$. The increase this represents in the Bjorken-x range over which charm may be studied in DIS is illustrated in figure 2 for two Q^2 ranges.

The upgraded FTD will also allow better measurements of the contribution of charm to photoproduction. Both HERA experiments have observed an excess over expectation of $D^\star$ mesons produced at the largest rapidities accessible with their central track detectors [15, 16]. The upgraded FTD will allow this measurement to be extended further into the forward region.

As the amount of data available increases, it will become possible to study b quark production in detail at HERA. Preliminary results using two methods to identify b events have been obtained by the H1 collaboration. The first method uses 2+1 jet events[2] containing muons. Monte-Carlo studies show that muons from b decays have a higher transverse momentum with respect to

[2]The 2 refers to the jets produced in the hard subprocess, the 1 to the proton remnant.

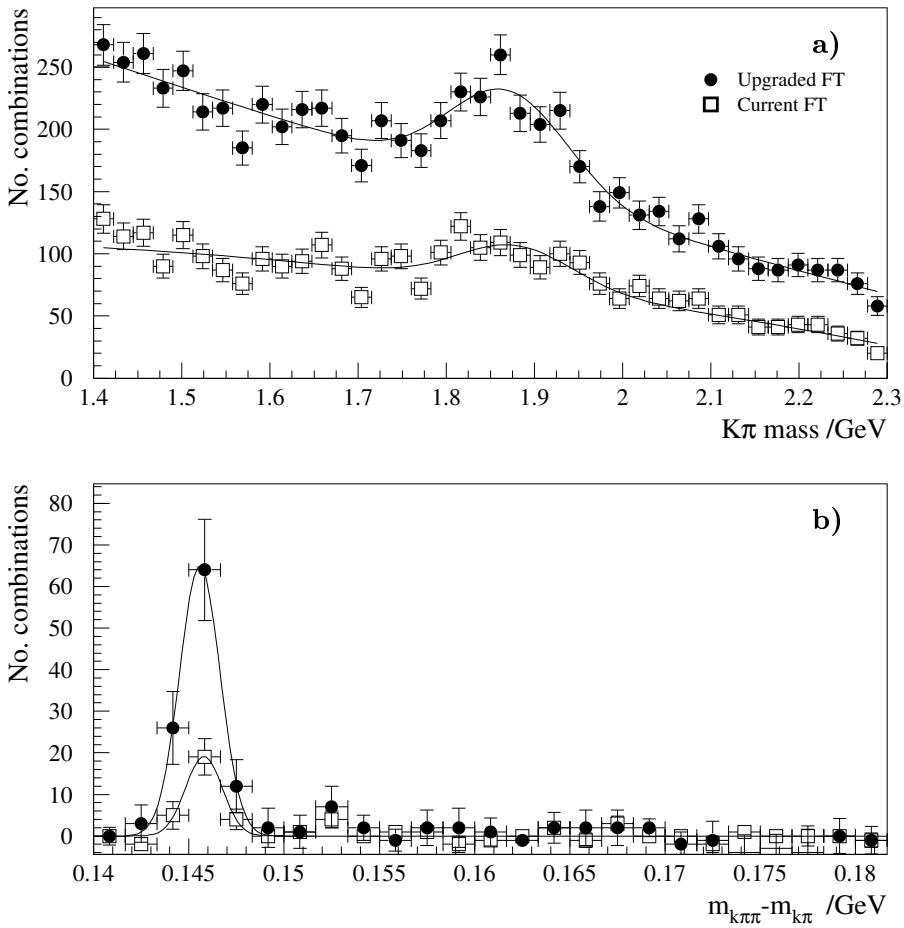

Figure 1: a) The $K\pi$ mass spectrum in DIS events in the range $Q^2 > 4\,\mathrm{GeV}^2$, $x > 0.007$ and $\theta_q < 30°$ requiring transverse momenta above 0.4 GeV/c for the K and π candidates.

Figure 1: b) The background subtracted Δm distribution in the kinematic region given above with the additional requirement that the $D^\star$ transverse momentum be greater than 2 GeV/c.

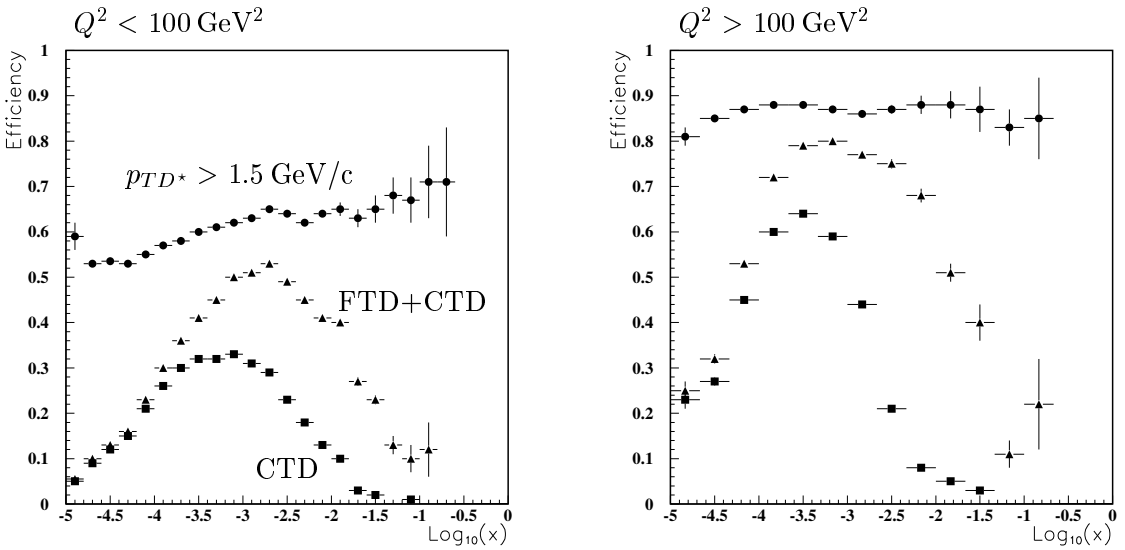

Figure 2: Shown is the proportion of DIS charm events containing a $D^\star$ with transverse momentum greater than 1.5 GeV/c (circles) in the ranges $Q^2 < 100\,\mathrm{GeV}^2$ and $Q^2 > 100\,\mathrm{GeV}^2$; the squares show the proportion of events in which the $D^\star$ is within the geometric acceptance of the CTD and the triangles this proportion for the combined FTD and CTD.

the jets with which they are associated than those from uds or c quark decays. This enables determination of the rate of b quark production. The second method uses events containing two like-charge muons. These are observed relatively frequently in b events. The first method give rise to an open b production cross-section which is a factor of more than five higher than leading order QCD expectation [17]. The second method confirms this result, albeit with large uncertainties. The increased efficiency for the determination of the momentum and charge of muons in the forward region provided by the FTD upgrade would particularly improve these measurements. For example, Monte Carlo studies made using AROMA [18], indicate that the efficiency for observing like-sign dilepton events would increase by a factor of about 2 with the upgraded FTD.

2.3.3 Other new QCD effects

The search for QCD instanton induced events would also benefit from the increased efficiency of the upgraded FTD. Instantons represent tunnelling transitions between degenerate vacua with different topological quantum numbers and are responsible for baryon number violating processes in the electroweak sector of the SM [19]. These transitions were originally thought to occur with unobservably small probabilities. However, it was recently realised that this may not be the case at high energies [20]. Electroweak instantons cannot be studied at HERA, but their QCD equivalents can. For these, the analogue of baryon number violation is chirality violation. The possible contribution of QCD instanton effects to DIS has been emphasised [21] and a two-loop calculation of the cross-section in DIS has recently been completed [22]. This suggests that such effects may already be present in the HERA data at a significant level. Possible search strategies for instanton induced events have been discussed [23]. Models of the final state produced in instanton induced events are still in a state of flux, but typical signatures include the production of large numbers of particles in a relatively narrow rapidity band and democratic production of all kinematically allowed quark flavours. This rapidity band can be covered in H1 using the CTD and the upgraded FTD, as illustrated in figure 3, which shows the expected rates of K^0 production in DIS with and without an instanton induced contribution as a function of pseudorapidity. The prediction for the rate due to instanton induced events was obtained using the currently available model, QCDINS 1.3 [24], which is based on the HERWIG [25] Monte Carlo program.

Searches for enhanced strangeness, charm and beauty production would profit from the increased efficiency of the upgraded FTD. The detection of charm and beauty is discussed above. The improvements in the detection of strangeness arise from the increased efficiency with which K^0_S decay products can be identified in DIS events following the upgrade. If a K^0 has a transverse momentum above 1 GeV/c, it is currently detected with an efficiency of less than 10% in the forward region. This increases to about 30% with the proposed upgrade. (The remaining loss of efficiency arises largely from the necessity of demanding that the decay vertex be removed from the primary interaction vertex in order to reduce combinatorial background.) The discovery of instanton induced effects would be of fundamental importance and every effort should be made to ensure that the H1 detector is optimally equipped for the search. As illustrated for the case of a search using the observed K^0 production rate, the FTD upgrade significantly improves the ability of H1 to make such discoveries.

A continuing discussion at HERA concerns the regions of validity of the QCD evolution schemes used in structure function calculations, such as those of BFKL [26] and DGLAP [27]. It has been established that inclusive measurements, *e.g.* $F_2(x, Q^2)$, are not sensitive to the differences in these schemes [28]. However, some evidence has been found for the necessity of including BFKL or BFKL-like evolution in studies of the hadronic final state; in particular the

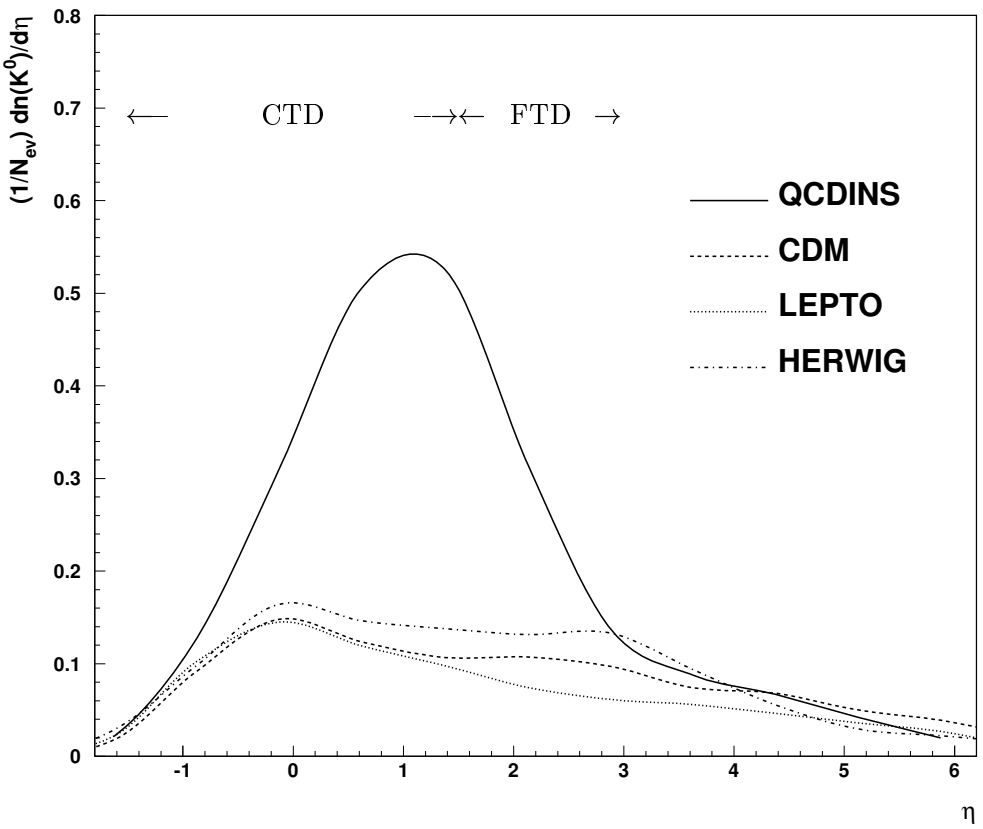

Figure 3: The number of K^0 mesons per DIS event produced in the range $10 < Q^2 < 70\,\mathrm{GeV}^2$ and $10^{-3} < x < 10^{-2}$ predicted by various models of DIS which do not include instanton induced events (broken lines) and by QCDINS which is a model of instanton events (solid line).

transverse momentum spectrum of forward going hadrons in low x DIS events is harder than expected in DGLAP based models [5], and the forward jet cross-section [29] and the rate of production of high energy forward π^0 mesons in DIS [30] are somewhat higher than DGLAP predictions. Studies of the first two of these topics would obviously benefit from improved FTD efficiency. In the last case complementary results have recently been obtained using the FTD to detect forward charged pions [31]. The measurement, shown in figure 4, is currently not competitive with that made using π^0 mesons. This is due to the large model dependent corrections that must be made to compensate for the poor, multiplicity dependent tracking efficiency, leading to the large systematic errors apparent in figure 4. This figure also shows the statistical and systematic errors expected using the current and the improved FTD following one years running after the HERA luminosity upgrade. These were determined using LEPTO 6.4 [14] and ARIADNE 4.08 [32] to calculate the necessary corrections and the resulting systematic error. Following the upgrade, the statistical errors on the measurement are negligible using both the current and the upgraded FTD. The improvements result largely from the removal of the dependence of the FTD efficiency on multiplicity provided by the upgrade.

As luminosity increases, it becomes possible to search for further novel QCD effects. The evolution schemes described above all result in an increasing parton density with decreasing x. This cannot continue indefinitely and, as is discussed in [33], parton recombination must start to occur when parton densities become sufficiently high. As in the case above, it is probable that structure function measurements alone are not sensitive to such effects. One way of observing phenomena associated with recombination is to study the rapidity correlations of the hadrons produced in DIS. As pointed out in reference [34], such measurements require that correlations over the largest possible rapidity range are studied, making necessary the combination of the CTD and the FTD in H1.

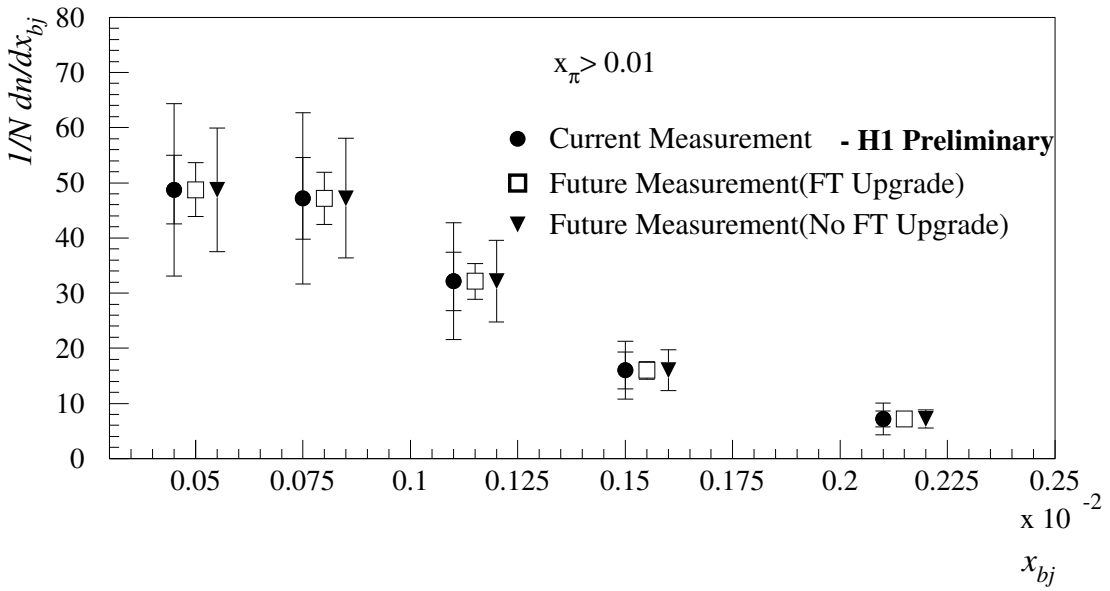

Figure 4: The current H1 measurement of the rate of forward $\pi^{\pm}$ production; the inner error bars indicate the statistical and the outer the systematic errors. Also shown are the expectations for future measurments with and without the FTD upgrade; the statistical error bars associated with these are smaller than the graph symbols.

The increase in luminosity will also allow the extension of studies of the fragmentation of the quarks struck in DIS to larger values of Q^2. These studies are performed in the current hemisphere of the Breit frame of reference[3], which in the presently accessible Q^2 and x range corresponds predominantly to the central region of the H1 detector [7]. As Q^2 rises, however, the region covered by the FTD contributes increasingly to the Breit frame current hemisphere and the majority of relevant particles are found in the FTD at the highest values of Q^2 and x.

The Modified Leading Log Approximation of QCD, coupled with the hypothesis of Local Parton Hadron Duality, makes interesting predictions concerning the behaviour of the hadron spectrum at low hadron energy [35]. H1 has observed the expected independence of the spectrum of hadrons in a jet on the energy of the parton from which the jet originated [7]; again, this study was performed in the Breit frame and if it is to be pursued to higher energy will require an increase in the efficiency of the FTD.

The upgrade of the FTD also brings advantages for the study of ep interactions in which the exchanged photon is essentially real, $Q^2 \approx 0$. At leading order, it is possible to distinguish two types of such photoproduction interactions. The first type are termed direct photon interactions. In these, the photon acts as a pointlike object, all of its momentum being involved in the scattering with the parton struck in the proton. In the second type, termed resolved photon interactions, the photon interacts as a hadron-like object; a parton from the photon, carrying a proportion x_γ of the photon's momentum, collides with a parton from the proton. In some photoproduction interactions, jets with large momenta transverse to the beam direction are produced. If there are two such jets, it is possible to determine x_γ, and measurements can be made of the structure of the photon [36]. As x_γ decreases, the jets are found increasingly in the forward direction, as is shown in figure 5. This figure was obtained using the HERWIG Monte Carlo and the GRV parton distribution functions for the both the photon [37] and the

[3]The Breit frame is the frame of reference in which the four-momenta of the incoming virtual photon and quark in quark parton model scattering processes are $(0,0,0,-Q)$ and $(Q/2,0,0,Q/2)$, respectively, the current hemisphere being that hemisphere into which the virtual photon is travelling.

proton [38]. Studies of the properties of hadrons in these jets, in particular measurements in the range $x_\gamma \lesssim 0.2$, benefit from the proposed upgrade. One such study, again of a prediction of the Modified Leading Log Approximation with the hypothesis of Local Parton Hadron Duality, is the dependence of the soft particle density on the colour charge in photoproduction events [39]. This requires the largest possible acceptance for charged particles to allow the study of soft particle production in both direct and resolved photon proton interactions over a large range of x_γ.

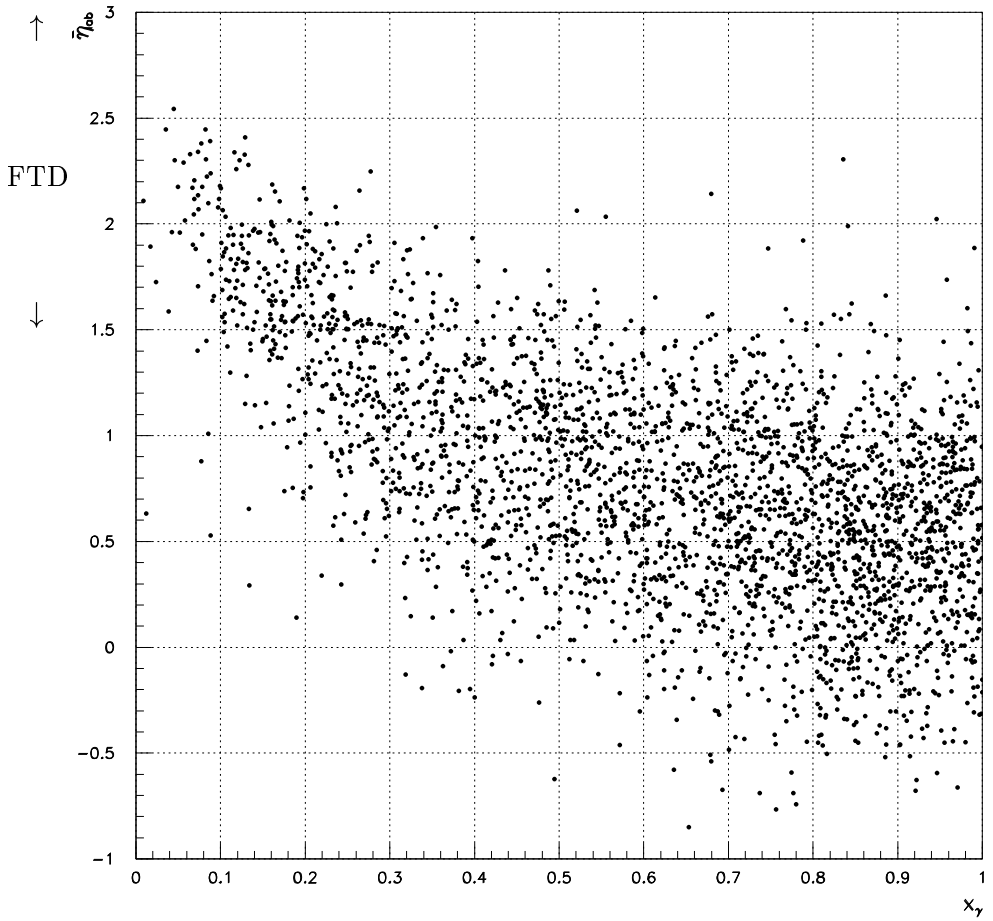

Figure 5: The mean jet pseudorapidity, $\bar{\eta}_{lab}$, in di-jet events in which both jets have a minimum transverse energy of 5 GeV and the jets are separated by less than one unit of pseudorapidity in the kinematic region $Q^2 < 4\,\mathrm{GeV}^2$ and $0.1 < y < 0.7$. Measurements of hadrons in the range $1.5 < \eta < 3.0$ are possible with the upgraded FTD.

The measurements described here form only part of the HERA physics programme following the luminosity upgrade; more information on the plans of the H1 collaboration can be found in reference [40].

3 The HERA upgrade

The HERA high luminosity upgrade requires that three superconducting magnets be installed within H1. The current H1 detector is shown in figure 6, in which the H1 coordinate system is also defined. One of the new superconducting magnets sits in a cryostat inside the FTD, as is shown in figure 7, the other two are located in the backward direction. The new magnets

are used to focus the beams more tightly at the interaction point, hence producing the desired increase in luminosity. The bending of the electron beam that occurs within the forward magnet causes synchrotron radiation to be produced within the H1 detector and a system of collimators has been designed to ensure that the detector is screened from this radiation as far as is possible. A new, elliptical, aluminium coated carbon-fibre beam pipe is also to be installed within H1 to satisfy the requirements of the beam optics and simultaneously allow the H1 central silicon tracker to be placed as close to the interaction point as is possible.

4 The current Forward Track Detector

The location of the FTD within the H1 detector is shown in figure 7 and the current FTD in more detail in figure 8. The sensitive volume of the FTD is located between $z = 1.34\,\mathrm{m}$ and $z = 2.54\,\mathrm{m}$ and covers the radial range $0.15 < r < 0.79\,\mathrm{m}$. The resulting angular range over which track measurements may be made is about $5^\circ < \theta < 25^\circ$, corresponding to the pseudorapidity range $3.1 > \eta > 1.5$. Tracks in the range $8^\circ < \theta < 18^\circ$ ($2.7 > \eta > 1.8$) pass through the entire sensitive volume of the FTD. The FTD consists of three supermodules. Each of these contains, in order of increasing z, a planar module, a multi-wire proportional chamber (MWPC) module, a transition radiator and a radial chamber. The FTD and the H1 detector are described in more detail in reference [41].

The planar modules are composed of three planar chambers. A planar chamber is illustrated in figure 8A and in more detail in figure 9. The planar chamber situated closest to the interaction point is made of 32 rectangular cells which each contain 4 vertical sense wires. These are spaced at 6 mm intervals along the z axis with a stagger of $\pm 300\,\mu\mathrm{m}$ in the x direction, which aids resolution of the left-right ambiguity. The second chamber, in order of increasing z, is similarly constructed but oriented with the wires at $+60^\circ$ to the vertical, the third with the wires at -60°. The wires are read out at one end via a pre-amplifier and a 104 MHz FADC. Subsequent analysis of the FADC signals allows determination of the charge deposited on a wire and the time, and hence distance in the drift direction, at which a particle passed the wire. The four wires in a planar chamber thus define a plane in space containing the path of the particle. The combination of two planes defines a line segment on the particle's path. If several particles pass through the chamber, many possible combinations of two planes result and the third plane must be used to resolve these "hodoscope" ambiguities to define a so-called "planar segment" on each of the tracks.

The radial chambers, as illustrated in figures 8D and 9, contain radially strung wires, sets of 12 of which are arranged along the z direction with an inter-wire spacing of 10 mm in 48 wedge shaped drift cells. The wires in one cell are connected at the inner hub with those in a cell displaced by 105° in ϕ. Each of the wires thus passes through two drift cells. They are read out at both ends using the same FADC system as for the planar chambers. Again, the drift coordinate of a track is determined by analysis of the FADC signals. The two-ended readout also allows the determination of the coordinate along the wire using charge division, and hence which of the two possible cells was crossed by a particle. The radial chambers define the plane in which a particle crossed the chamber accurately in the drift direction but much less so in the wire direction as the charge division coordinate is much less accurately measured. These measurements define a "radial segment" on a track.

The rear face of the radial chambers, adjacent to the transition radiators, consists of a thin mylar window outside which are aluminium drift field cathode electrodes attached to a low mass rohacell support. This structure is transparent to x-rays. Its purpose is to allow the transition radiation generated by high energy electrons crossing the foils in the transition radiators to enter the radial chamber. These can then be detected on the first wires of the chamber, if an appropriate gas mixture is used, aiding the separation of electrons from pions which do not generate transition radiation at the energies relevant here [42].

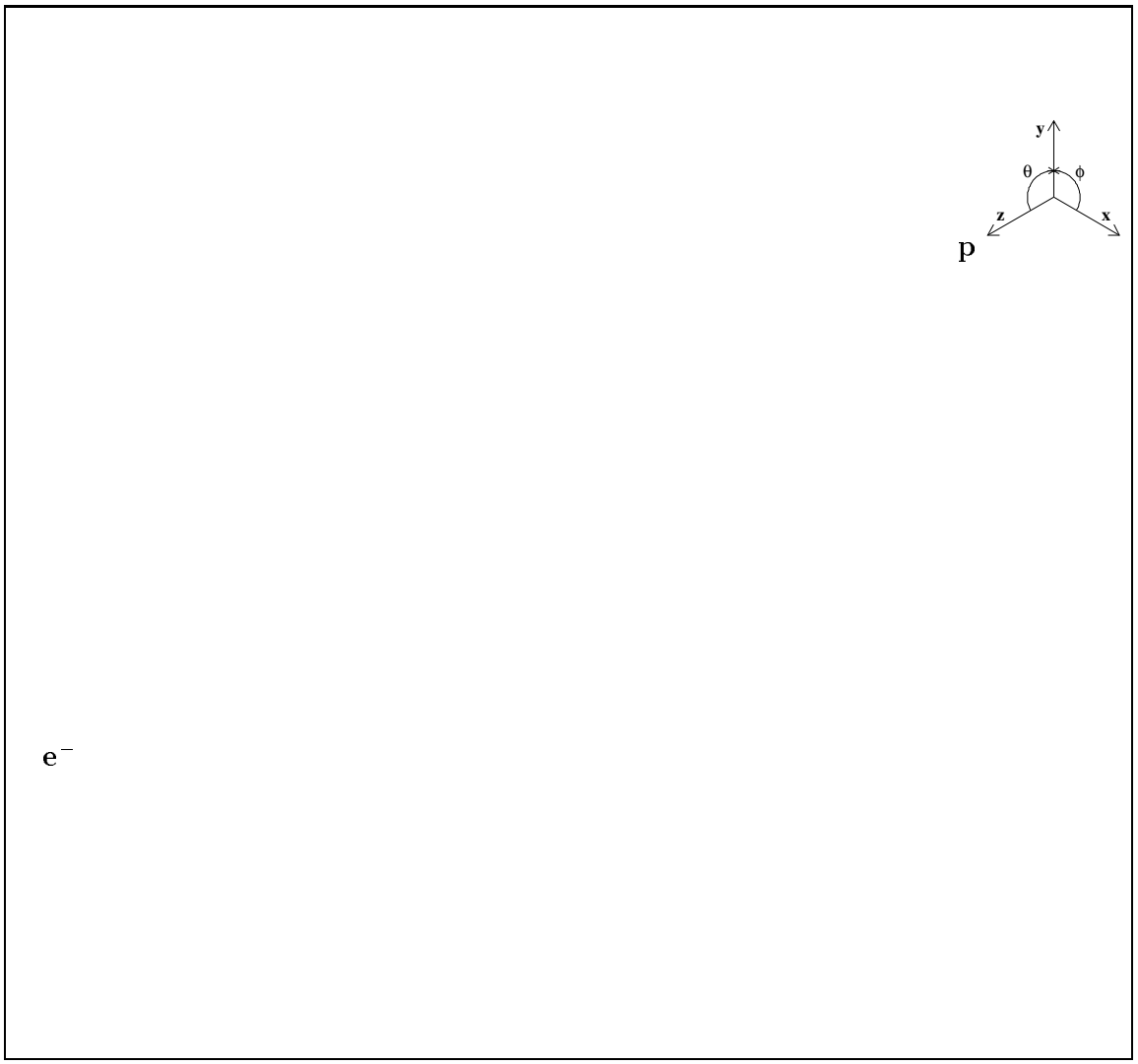

1	Beam pipe and beam magnets	9	Muon chambers
2	Central tracking device	10	Instrumented iron yoke
3	Forward tracking device	11	Forward muon toroid
4	Electromagnetic LAr calorimeter	12	Backward calorimeter (SpaCal)
5	Hadronic LAr calorimeter	13	PLUG calorimeter
6	Superconducting coil (1.15 T)	14	Concrete shielding
7	Compensating magnet	15	Liquid argon cryostat
8	Helium supply for 7		

Figure 6: The H1 detector showing the position of the Forward Track Detector, denoted 3, and illustrating the H1 coordinate system, the origin of which is at the nominal interaction point.

4.1 Track finding and fitting in the FTD

The identification of tracks in the FTD starts with a search for groups of three or four hits in each of the planar chambers which are consistent with forming a straight line. These are referred to as "clusters". Sets of three clusters in the planar chambers within a planar module are then

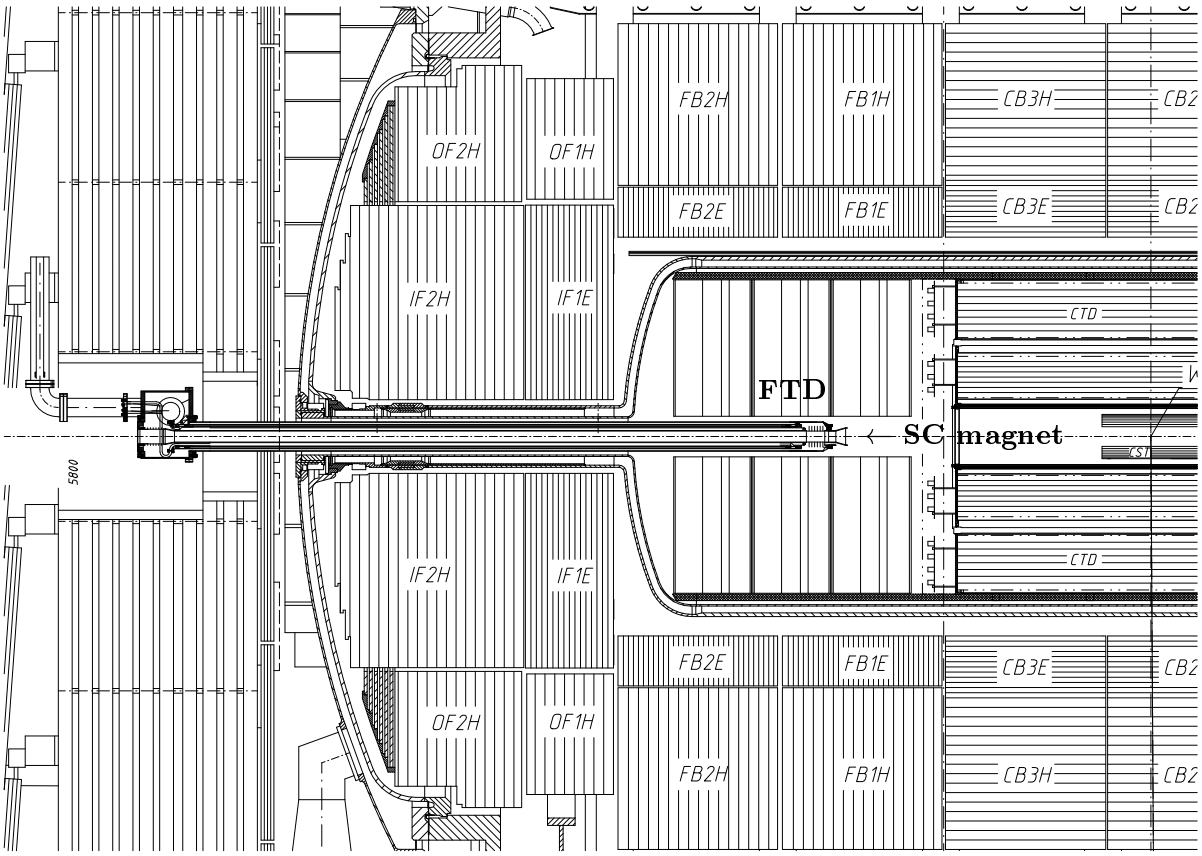

Figure 7: The superconducting magnet with accompanying cryostat to be placed inside the forward region of the H1 detector.

combined to form planar segments. Two qualities of planar segment are distinguished: "primary" planar segments, for which all three planes are defined by three or four hits, and "secondary" planar segments for which one of the planes is defined by only one or two hits. The segment finding procedure used is hierarchical. The primary segments are found first, any conflicts over which clusters belong to which segment being resolved by choosing the combination giving the best quality of fit, and the clusters associated with them are removed from the procedure. A search for secondary segments is then made.

Radial segments are identified by searching for all possible triplets of adjacent hits within a radial chamber that are consistent with lying on a straight line. In a second step triplets are joined if they are consistent with lying on a straight line and are separated by not more than one wire on which there is no hit.

The above segments are then linked to form tracks if they are consistent with lying on a helical path. A Kalman filtering technique is used to determine the optimum track parameters and hence the momentum, distance of closest approach to the vertex, *etc.* This method allows for the exclusion of hits found to be incompatible with belonging on the track, as well as the inclusion of hits which belong on the track but were missed by the above pattern recognition procedure. More information on all these procedures is given in reference [43].

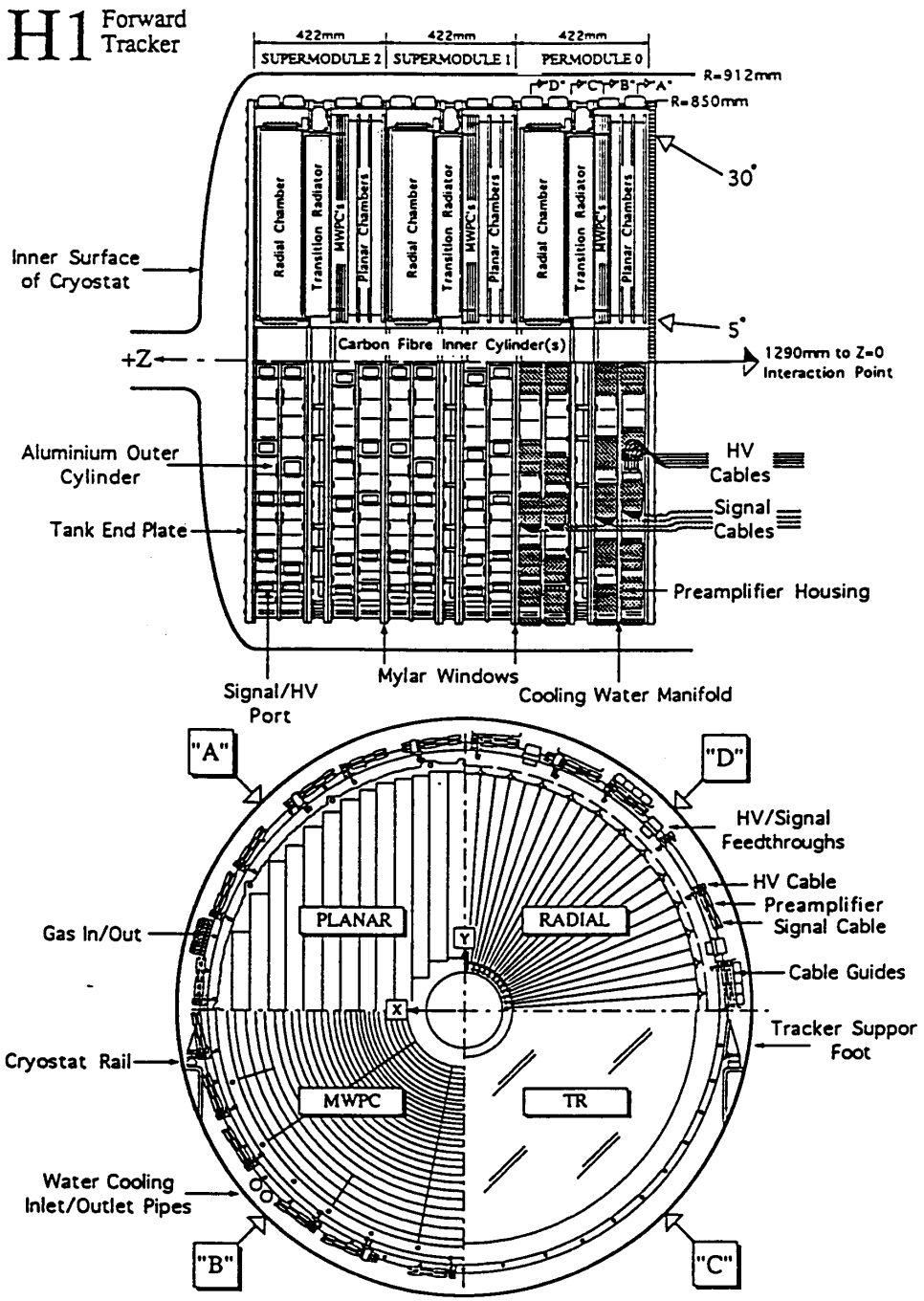

Figure 8: The forward track detector currently installed in the H1 detector showing the planar chambers, the multi-wire proportional chambers, the transition radiators and the radial chambers.

4.2 Current FTD performance

4.2.1 Hit and segment finding efficiencies

The efficiencies of the hit finding in the radial and planar chambers, including the effects of the chamber, readout and subsequent analysis, have been studied using both *ep* and cosmic ray data. The methods used are described in reference [43]. The results show that the efficiency of the planar wires is greater than 98%, where the efficiency is defined to be the probability that

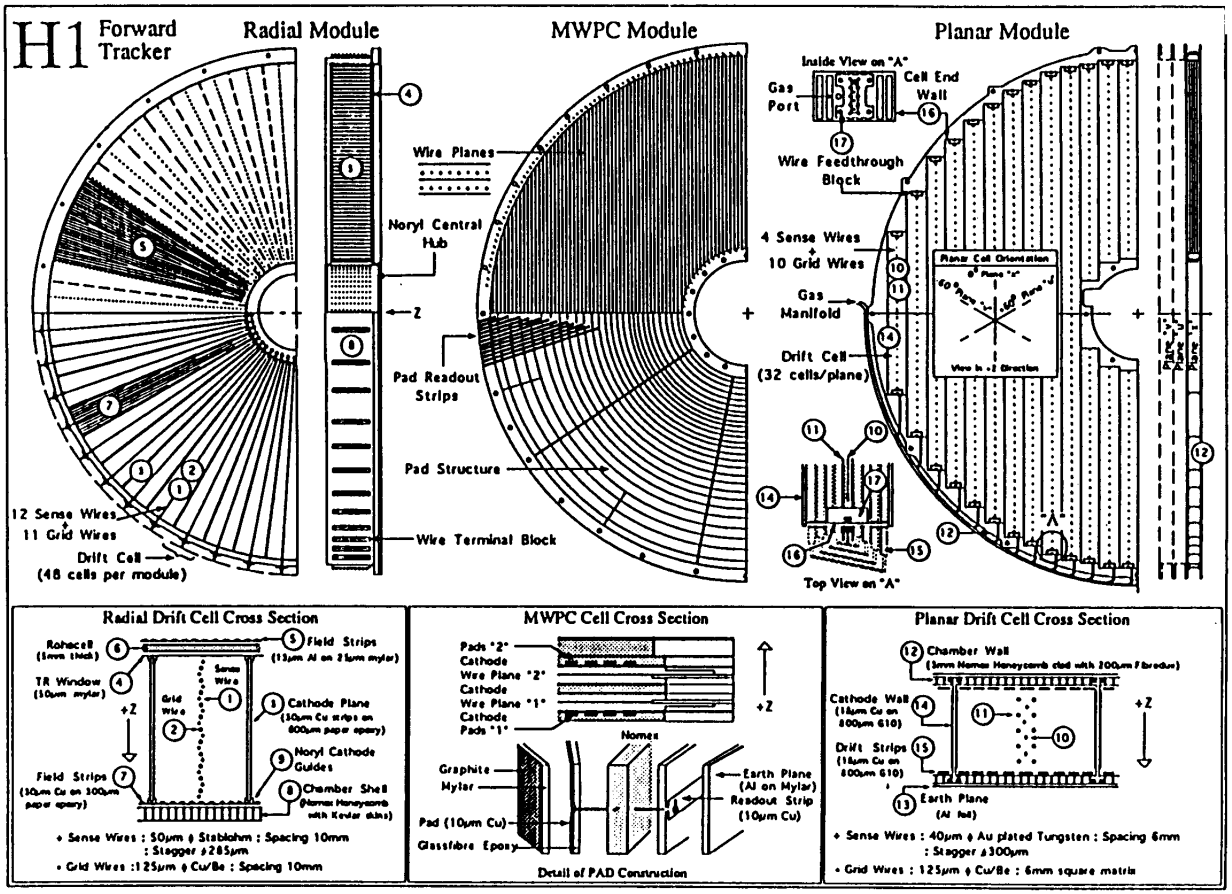

Figure 9: The radial, planar and multiwire proportional chambers of the current Forward Track Detector.

a hit is found at the expected position on the fourth wire of a planar cell if three hits are found in a straight line on any combination of the other three wires of the cell. For the most forward 10 wires of the radial chambers (those furthest from the mylar window), the equivalent number is 93%. The efficiency of the two wires closest to the mylar window is in general lower than this. These wires suffer from reduced gain, and hence efficiency, shortly after turn-on due to the build-up of charge on the mylar window which influences the electric field configuration at the rear of the chamber [44].

The above wire efficiencies suggest that the efficiency for identifying planar and radial segments on a track should be nearly 100%. However, studies of *ep* collision data reveal this is not the case. For example, if well-measured tracks in low multiplicity events observed in the rearmost and foremost FTD supermodule are interpolated into the central supermodule, for each of the central planar chambers it is observed that the probability that a cluster was identified on the track is only 89%. This number does not depend on which of the planar chambers is studied. In addition, the probability that there are two or three missing clusters is compatible with the chambers being independent of one another; that is, the loss of a cluster in one planar chamber does not influence the probability that a cluster is lost in the adjacent planar chambers.

As planar segments can only be formed when clusters are observed in all three planar chambers in a module, the segment efficiency expected from this observation drops to 70%. This is compatible with the number of segments observed on the interpolated tracks in the above low multiplicity events.

Track selection criteria	Efficiency (%)	Resolution (GeV^{-1})	Prop. good tracks
2R or 1P(p or s)	95	0.076	50
1P(p)	77	0.070	66
1P(p) and V	70	0.068	75
1P(p) and (1P or 1R) and V	66	0.063	89
1P(p) and (1P or 1R) and V and F	60	0.057	92

Table 1: Influence of track selection criteria on the quality of forward tracks with $p > 1\,\mathrm{GeV/c}$ in the angular range $8^\circ < \theta < 18^\circ$: 1R indicates a minimum of 1 radial segment required; 1P(s) a minimum of one secondary planar segment; 1P(p) a minimum of one primary planar segment; V indicates that the track was required to originate from the primary vertex, within errors, and F that a reasonable fit quality was required. The resolution is given in terms of the FWHM of the distribution $\frac{q_{\mathrm{meas.}}}{p_{\mathrm{meas.}}} - \frac{q_{\mathrm{true}}}{p_{\mathrm{true}}}$. This distribution is approximately Gaussian, but has large tails, so in addition the proportion of good tracks is given, *i.e.* the proportion for which $|\frac{q_{\mathrm{meas.}}}{p_{\mathrm{meas.}}} - \frac{q_{\mathrm{true}}}{p_{\mathrm{true}}}| < 0.25$.

A possible explanation for some of the effects causing the cluster loss in the planar chambers is the confusion caused when the track passing through the chamber produces a δ-ray in the chamber wall, which then traverses the chamber, spiralling about the magnetic field direction, before being absorbed at the opposite wall or reflected back into the chamber. As the tracks are at small polar angles, and the magnetic field is directed along the z direction, the track and δ-ray remain in close proximity. Electrons require a minimum kinetic energy of around 50 keV to cross an entire planar chamber, when account is taken of the typical path followed. The radius of curvature of their path in the H1 magnetic field is then of the order of 1 mm. The δ-rays thus produce a swathe of ionisation of width typically 2 mm about the hadron track, making it unlikely that the ionisation due to the hadron can be disentangled in the confused signal.

Simulations of the planar chambers were performed using GEANT [45] with the energy cut-off down to which δ-rays are generated lowered from the default 1 MeV to 10 keV. It was observed that the probability per hadron per planar chamber of a δ-ray being produced which traversed the chamber was 12%, a result confirmed using a Monte Carlo routine written specifically to simulate δ-ray production in the planar chambers. The rate of occurrence of such effects is thus of the right order to explain the above observations on cluster loss.

4.2.2 Hadron detection efficiency

The efficiency with which hadrons are detected in the current FTD depends on the stringency of the criteria used in the track selection. These criteria also affect the momentum resolution attained. Table 1 shows these quantities for various selection criteria for tracks in the angular range $8^\circ < \theta < 18^\circ$. The figures are for tracks with momenta above 1 GeV/c in low Q^2 DIS events. Due to the steeply falling momentum spectrum, the majority of tracks in the sample have momenta only slightly above 1 GeV/c and the momentum resolution for good tracks is dominated by the effects of multiple scattering. The physics analyses described above all require a track quality only obtainable when tracks are required to be formed from at least one primary planar segment and one further segment and to be compatible with coming from the ep interaction point. In addition, it is necessary to demand that the track fit be reasonable. The resulting track selection efficiency is 60%[4]. This number decreases to 42% for the highest Q^2 events as in these the jet of particles associated with the struck quark is often very dense. The reason this number is lower than is desirable is largely the planar segment finding efficiency, in particular the efficiency for finding high quality primary planar segments.

[4]This figure is corrected for the effects of dead wires *etc.* and represents the best possible efficiency obtainable with the existing FTD; the actual efficiency is currently about 50% in high multiplicity events.

The above discussion describes how effects which may be attributable to δ-rays depress the planar segment finding efficiency. The lack of redundancy in the planar modules causes a further problem. As the multiplicity increases, spurious solutions to the hodoscope ambiguities mentioned above occur more frequently. These "ghost" segments can result in the loss of up to three true segments if the procedure for selecting the optimal set of segments in the planar module picks a combination including a ghost. Above a multiplicity of about 15, this effect causes a loss of segment finding efficiency, as is illustrated in reference [43]. This is compounded as the multiplicity increases by the increasing frequency with which random combinations of three or four hits within a planar chamber are combined to form incorrect clusters. These enter the segment finding procedure and increase the chance that ghost segments appear.

The above problems are made worse by the large number of particles produced in secondary interactions in the material between the CTD and the FTD and in the beam pipe and associated collimators. The material of the CTD end wall, including the central jet chamber electronics and associated cables, amounts to about $0.5\,X_0$. Each charged pion emerging from the primary vertex is accompanied on average by one photon from the decay $\pi^0 \to \gamma\gamma$ and these photons pass through the CTD end wall, typically one of them producing an electron-positron pair. Adding to this the particles produced in secondary interactions in the collimator and beam pipe, gives an average of four secondary particles for every primary hadron in the FTD. Provided that well-measured tracks constrained to originate from the primary vertex are used, this background can largely be excluded in physics analyses, but the resulting loss of efficiency restricts the topics that can be studied using the FTD.

5 Proposed upgrade

The time available for the upgrades described here limits the scale of the modifications that can sensibly be attempted. Those proposed can be made within the given time and produce the required improvement in the performance of the FTD.

The basic strategy of the proposed FTD upgrade is as follows:

- Create space within the FTD by removing those components which will not make a significant contribution to high Q^2 physics.
- Add three extra planar chamber orientations to aid resolution of the hodoscope ambiguities and to decrease the sensitivity to any inefficiencies.
- Increase the number of sense wires in the new planar chambers to aid resolution of the left-right ambiguity and increase the accuracy of the segment measurements.

5.1 Creation of space for new chambers

The components that can be removed from the FTD without compromising high Q^2 physics are the MWPCs and the transition radiators. The MWPCs are unlikely to survive a further 7 or more years of luminosity. They are currently used to provide the z-vertex trigger [46] for events with only forward tracks and to provide the forward ray trigger, which is designed to be used in conjunction with information from the liquid argon calorimeter (LAr) trigger system. These trigger functions will become largely superfluous when the proposed new central inner multi-wire proportional chambers (CIP) and associated z-vertex trigger are installed [47]. A scintillator trigger, discussed below, will be added to ensure that full trigger capability is maintained.

The transition radiators were designed, in conjunction with the radial chambers, to provide enhanced electron identification in the forward region [42]. However, electrons must traverse about $0.5\mathrm{X}_0$ of material before entering the FTD and are thus accompanied by electrons and positrons generated in an electromagnetic shower in that material about 80% of the time. A high Q^2 event in which this has occurred in shown in figure 10. The transition radiation signal is not of value in this situation.

5.2 Construction of new planar chambers

The above measures create space for the major part of the proposed upgrade, the construction and insertion of new planar chambers. It is proposed to build one new planar chamber per planar module and rearrange the existing planar chambers so that the sense wires of the four planar chambers in each module are oriented at $\phi = +60°$, $-60°$, $90°$ and $0°$, in order of increasing z. How this may be achieved is discussed in the following and the expected resulting improvement in performance evaluated. The costs are estimated, as is the effort required to build and install the new components.

The proposed new planar chambers are illustrated in figure 11. The design is similar to the current planar chambers, but advantage has been taken of the availability of improved materials to reduce the amount of material in the chambers to minimise the effects of multiple coulomb scattering. In particular the thickness of the G10 used on the inner faces of the chamber's honeycomb end plates has been reduced, as has the thickness of the copper cathodes and HV distribution bus. Studies of the desirability of using paper-epoxy rather than G10 are underway. The thickness of the G10 and copper cathode planes between cells has also been reduced. The net effect of the efforts to minimise the material in the new planar chambers is approximately to halve the number of radiation lengths they present to a particle traversing the FTD; each new chamber has a thickness of $1\%\,\mathrm{X}_0$.

A further improvement is that the number of wires per orientation is increased from the current four to six. This reduces the number of spurious clusters found in the chamber, arising for example due to the incorrect resolution of the left-right ambiguity, and increases the accuracy of the determination of the position and orientation of the planes that make up a segment.

The new planar chambers are of 5.6 cm smaller radius than the current design and thus contain 30 drift cells rather than 32. This enables the insertion of the chambers in the reduced radius sections of the gas tank at the positions currently occupied by the transition radiators, as is illustrated in figure 12. This then leads to an upgraded FTD as shown in figure 13. The redundancy the new planar chambers provide allows the resolution of more of the ambiguities in finding planar segments. Pattern recognition is further aided by the increased proximity of the radial and planar chambers. The distances over which segments need to be projected in the linking procedure are significantly reduced.

5.3 Forward trigger

The removal of the MWPCs destroys the current forward ray trigger. This will be largely replaced by the new CIP z-vertex trigger, but the very forward region, $\theta < 12°$, will not be covered. We propose to add a scintillator trigger to remedy this situation. The trigger, to be inserted at $z \approx 2.65\,\mathrm{m}$, *i.e.* the front of the FTD, consists of two sections. The first is composed of an annulus of fast scintillator surrounding the beam pipe. It is split into four sections each of which is read out by a photomultiplier. The fast signals that this provides will facilitate proton satellite bunch corrections, increasing the accuracy of the H1 luminosity measurement.

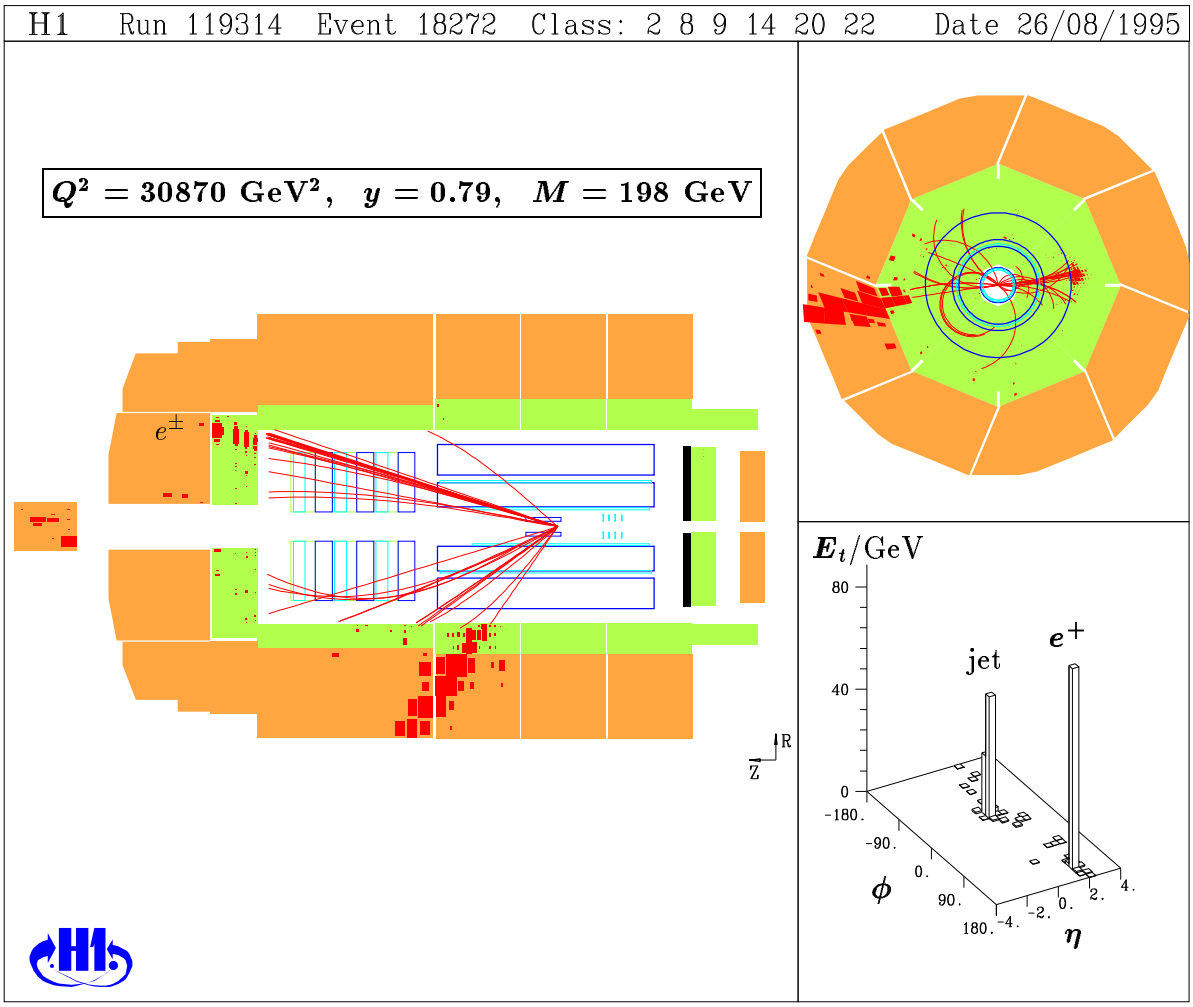

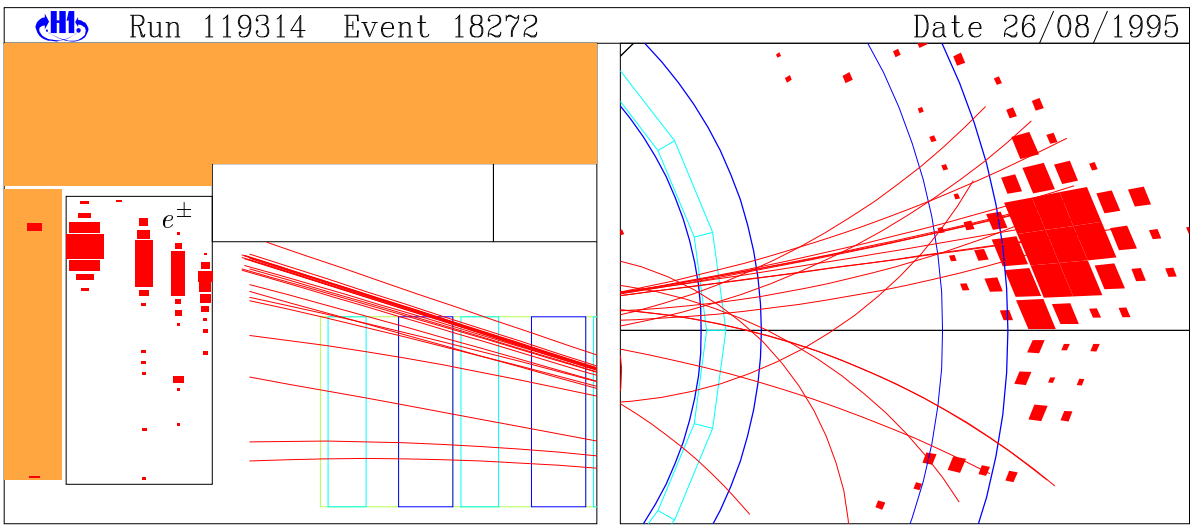

Figure 10: A high Q^2, high x event in which the scattered lepton has showered in the material between the FTD and the CTD.

Surrounding this is a larger disc of scintillator, split into two sections radially and 16 azimuthally, each section being read out using vacuum photo-triodes. This scintillator is matched to the liquid argon calorimeter trigger "big-tower" geometry and, in coincidence with the calorimeter, will allow improved triggering on forward going tracks. In addition, in conjunction with the CIP, it will provide a cosmic ray trigger which will be useful for the testing and calibration of the FTD. A small prototype of the above system has been installed in H1 and will be tested during the 1998 HERA running.

5.4 Further improvements to the FTD

The rohacell onto which the aluminium drift electrodes at the rear of the radial chambers are attached has shrunk with time, probably as it has lost moisture in its extremely dry surroundings. Some of the electrodes are wrinkled and it is feared that this may lead to voltage breakdown. We propose to replace the rohacell and associated electrodes with G10 or paper epoxy and copper electrodes to ensure this does not occur.

5.5 Expected performance

Monte Carlo studies have been made of the performance of the proposed forward track detectors. High Q^2 events were generated using the LEPTO 6.4 program [14] and passed through a GEANT based simulation of the detector. The resulting tracks were studied in the three super-modules of the FTD. Making the conservative assumption that the clusters in the new 6 wire planar chambers are identified with the same efficiency as those in the current 4 wire chambers, planar segments consisting of four clusters were identified. The number of hodoscope ambiguities associated with these is negligible. The clusters forming these segments were then removed from the segment finding procedure and a search for segments containing three clusters was made. The effect of the upgrade is to introduce redundancy to this segment finding procedure. The necessity of finding all three possible clusters on a segment has been removed; it becomes sufficient to find three of a possible four. The procedure used to identify radial segments was as described for the current detector. Tracks were then formed by linking these segments.

Forward tracks were required to be composed of at least two segments, one of which was a planar segment. The resulting efficiency for hadron detection in the angular region $8^\circ < \theta < 18^\circ$ was found to be 42% for the current FTD. The efficiency of the upgraded FTD was found to be 91%. As marked as the increase in efficiency is the increase in track quality. Only 37% of the tracks found by the current FTD have two or more planar segments associated with them. Following the upgrade, this number becomes 72%.

The effects of the HERA upgrade on the FTD are:

1. To increase the number of synchrotron radiation hits registered from typically less than one per bunch crossing to a little under ten per bunch crossing.

2. To increase by about 10% the number of tracks scattered into the FTD resulting from secondary interactions of particles produced in electron-proton collision.

3. To produce some non-uniformity of the magnetic field in the region close to the superconducting magnet within the FTD.

4. To increase the number of off-momentum electrons interacting in the beam pipe within the FTD and generating showers of particles which enter the FTD.

The first of the above does not significantly affect the FTD. The second causes a degradation of the tracking efficiency in the current FTD, due to the above-described multiplicity dependence of the efficiency, but has almost no effect on the performance of the upgraded FTD because of the added redundancy. Final figures on the stray fields outside the superconducting magnets are not yet available, but as long as the strength of these fields in the tracking region can be kept below about 10 ... 20 mT, the third of the above points will not cause a problem.

Point four above seems currently to be the most serious. The off-momentum electrons under consideration are generated in collisions between electrons and the remaining gas molecules in the beam pipe. Currently, these pass through the H1 and ZEUS detectors and are swept out of the beam by the HERA magnets. The insertion of a dipole magnet into the experiments means that some of these off-momentum electrons will be swept out of the beam within the detectors and interact in the beam pipe. The rate of such interactions is expected to be about 60 kHz [48]. On average, the off-momentum electrons carry about 50% of the nominal electron energy and they will thus cause extensive electromagnetic showers. This poses a severe threat to the operation of tracking detectors. There are two problems, one immediate and the other longer term. The immediate problem is the large number of secondary tracks, which will make identifying tracks associated with primary interactions difficult. The maximum drift time in the planar chambers is about 1 μsec; the rate of 60 kHz thus implies that the planar chambers will contain tracks from showers generated by off-momentum electrons in about 5% of recorded events. The situation in the radial chambers is similar. The long term problem arises due to the significant radiation load resulting from the off-momentum electron background. Doses of about 100 krad/year have been estimated for components close to the beam [48]. Further study of this problem is necessary, but it would appear that ways of reducing this background by a significant factor must be found.

5.6 Required resources

The cost of the FTD upgrade is DM 378 000 plus 13 man-years of effort, 6 of which will be provided through the UK universities and the remainder through the Rutherford and Appleton and the Daresbury Laboratories. To achieve the above cost it has been assumed that cables and FADC units currently in use on the FTD are re-used. The consequences of this are discussed below. A more detailed breakdown of the costs is given in table 2.

The FADCs and internal and external cables which are assumed to be re-used are those through which the rearmost four wires of each of the radial chambers are read out. As mentioned above, two of these wires suffer from reduced efficiency due to the charging of the radial chamber's mylar window. The above measure thus effectively results in the loss of two of ten good radial wires. This does impair slightly the performance of the upgraded FTD, but MC studies indicate the effect is small; a loss of efficiency of $< 1\%$ is expected. The resulting saving in cost is considerable: the FADC units required to equip the new planars would cost DM 432 000 (DM 508 000 including VAT at 17.5%); the external cables, *i.e.* those from the cable distribution area (CDA) to the electronics rucksack, would cost DM 135 000 (DM 159 000); and the re-usable internal cables, *i.e.* those from the FTD to the CDA, would cost DM 18 000 (DM 21 000). The total saving due to is this DM 585 000 (DM 687 000).

5.7 Project organisation

This project was approved by the UK's Particle Physics Experiments Selection Panel (PPESP) at the end of May 1998 and funded to the tune of DM 390 000. The overall schedule for the project is as illustrated in figure 14.

Item	Individual cost	Quantity	Total	Comments
Clean room	36 000	1	36 000	$6 \times 4\,\mathrm{m}^2$
Surface tables, jigs etc.	24 000	1	24 000	
New planar chambers	60 000	3	180 000	3 new planars needed
Water and gas system changes	3 000	1	3 000	
New feedthroughs	600	45	27 000	
Shipping costs	3 000	1	3 000	UK-DESY
Internal cables	9 000	3	27 000	Re-use radial/new cables
External cables	0	3	0	Re-use radial cables
Pre-amplifiers	300	72	22 000	Manufactured complete
HV cables	0	0	0	Re-use MWPC cables
FADCs	0	36	0	Re-use radial units
Crates	0	0	0	Exist
Column total			322 000	
Plus VAT			378 000	17.5%

Table 2: Break down of costs for construction and installation of 3 new planar chambers and re-orientation of existing planar chambers, units are German Marks.

The time critical phase of the project occurs during the HERA shutdown. Two months of work are necessary in the North Hall before the FTD can be removed from H1. Following this a minimum of three months are necessary to dismantle the current FTD, insert the new planar chambers, carry out the modifications to the radial chambers and re-assemble the FTD, carrying out the necessary tests at each stage. Current ideas on the schedule for this work are shown in figure 15. These require that six technicians work on the FTD during a large proportion of the HERA shutdown. Note that clean room space will be required at DESY during this period.

6 Request to the Physics Review Committee

Much physics requiring the efficient detection of charged particles in the forward region of the H1 detector has yet to be studied in detail. The data for such studies will become available following the proposed HERA luminosity upgrade in the year 2000. Simultaneous improvement of the H1 Forward Track Detector (FTD) would increase the discovery potential of H1 and allow more efficient exploitation of these data, leading to significant improvements in the statistical and systematic errors of many measurements. An upgrade programme for the FTD is outlined in this document. Given the tight schedule, this relies on using chambers similar to those in the current FTD to obviate the need for long test programmes. The proposal is to add three new planar chambers to the FTD and re-orientate the existing planar chambers. The necessary funding, amounting to DM 378 000, has been made available by the UK's Particle Physics and Astronomy Research Council. The total manpower required to build the new chambers, install them within the FTD and commission the detector is 13 man-years of which 7 man-years of technical effort are to be provided by the Rutherford and Appleton Laboratories and the Daresbury Laboratory; the remainder will be provided through the Universities of Birmingham, Lancaster, Liverpool and Manchester and the Queen Mary and Westfield College of the University of London.

The upgrade yields significantly improved hadron detection efficiency over that achievable with the current detector. We therefore request that the Physics Review Committee support this effort to improve the forward tracking performance of the H1 detector.

References

[1] Proc. of "Future Physics at HERA" workshop, Hamburg 1996, ed.s G. Ingelman, A. DeRoeck and R. Klanner, Vol. 2, page 1133.

[2] C. Adloff *et al.* (H1 Collaboration) Nucl. Phys. **B470** (1996) 3.

[3] S. Aid *et al.* (H1 Collaboration) Nucl. Phys. **B497** (1997) 3.

[4] T. Ahmed *et al.* (H1 Collaboration) Phys. Lett. **B338** (1994) 507;
S. Aid. *et al.* (H1 Collaboration) Nucl. Phys. **B472** (1996) 3.

[5] C. Adloff et al. (H1 Collaboration), Nucl. Phys. **B485** (1997) 3.

[6] "The evolution of inclusive charged particle spectra with Q^2 in ep interactions at HERA", H1 Collaboration, To appear in Proceedings of the International Europhysics Conference on High Energy Physics, Aug. 1997, Jerusalem, Israel.

[7] C. Adloff *et al.* (H1 Collaboration), Nucl. Phys. **B504** (1997) 3.

[8] C. Adloff *et al.* (H1 Collaboration), Zeit. Phys. **C74** (1997) 191.

[9] J. Breitweg *et al.* (ZEUS Collaboration), Zeit. Phys. **C74** (1997) 207.

[10] C. Adloff *et al.* (H1 Collaboration), Nucl. Phys. **B472** (1996) 32.

[11] J. Breitweg *et al.* (ZEUS Collaboration), Phys. Lett. **B407** (1997) 402.

[12] J.J. Aubert *et al.* (EMC Collaboration), Nucl. Phys. **B213** (1983) 31.

[13] S.J. Brodsky *et al.*, Phys. Lett. **B93** (1980) 451; Phys. Rev. **D23** (1981) 2745;
Phys. Rev. **D52** (1995) 6285.

[14] G. Ingelman, Proc. of the "Physics at HERA" workshop, ed.s W. Buchmüller and G. Ingelman, Hamburg (1991), Vol. 3 page 1366.

[15] C. Adloff *et al.* (H1 Collaboration), Zeit. Phys. **C72** (1996) 593.

[16] J. Breitweg *et al.* (ZEUS Collaboration), Phys. Lett. **B401** (1997) 192.

[17] G. Tsipolitis, to appear in Proc. of the 6^{th} Int. Conf. on DIS and QCD, DIS98, Brussels, April 1998.

[18] G. Ingelman, J. Rathsman and G.A. Schuler, DESY preprint, DESY 96-058 (1996), and hep-ph/9605285.

[19] G. 't Hooft, Phys. Rev. **D14** (1976) 3432.

[20] A. Ringwald, Nucl. Phys. **B330** (1990) 1;
O. Espinosa, Nucl. Phys. **B343** (1990) 310.

[21] I. Balitsky and V. Braun, Phys. Lett. **B314** (1993) 237.

[22] A. Ringwald and F. Schrempp, to appear in Proc. of the 6^{th} Int. Conf. on DIS and QCD, DIS98, Brussels, April 1998.

[23] A. Ringwald and F. Schrempp, DEST preprint, DESY-94-197 (1994);
M.J. Gibbs, A. Ringwald and F. Schrempp, DESY preprint, DESY-95-119 (1995);
M. Gibbs, T. Greenshaw, D. Milstead, A. Ringwald and F. Schrempp, Proc. of "Future Physics at HERA" workshop, Hamburg 1996, ed.s G. Ingelman, A. DeRoeck and R. Klanner, Vol. 1, page 509.

[24] M.J. Gibbs, A. Ringwald and F. Schrempp, DESY preprint, DESY-95-119 (1995).

[25] G. Marchesini *et al.*, Comp. Phys. Comm. **67** (1992) 465.

[26] V.S. Fadin, E.A. Kuraev and L.N. Lipatov, Sov. Phys. JETP **45** (1977) 199;
Ya. Fadin and L.N. Lipatov, Sov. J. Nucl. Phys. **28** (1978) 822.

[27] V.N. Gribov and L.N. Lipatov, Sov. J. Phys. **15** (1972) 438; Ibid. 675;
L.N. Lipatov, Sov. J. Phys. **20** (1975) 94; G. Altarelli and G. Parisi, Nucl. Phys. **126** (1977) 298; Yu. L. Dokshitzer, Sov. Phys. JETP **46** (1977) 641.

[28] A.J. Askew, J. Kwiecinski, A.D. Martin and P.J. Sutton, Phys. Lett. **B325** (1994) 21;
M. Glück, E. Reya and A. Vogt, Zeit. Phys. **C67** (1995) 433.

[29] S. Aid *et al.* (H1 Collaboration), Phys. Lett. **B356** (1995) 118.

[30] "Forward π^0 and production at HERA", H1 Collaboration, To appear in Proceedings of the International Europhysics Conference on High Energy Physics, Aug. 1997, Jerusalem, Israel.

[31] T. Wengler, to appear in Proc. of the 6^{th} Int. Conf. on DIS and QCD, DIS98, Brussels, April 1998.

[32] L. Lönnblad, Comp. Phys. Comm. **71** (1992) 15.

[33] L.V. Gribov, E.M. Levin and M.G. Ryskin, Phys. Rep. **C100** (1983) 1.

[34] K. Charchula and E.M. Levin, Proc. of the "Physics at HERA" workshop, ed.s W. Buchmüller and G. Ingelman, Hamburg (1991), Vol. 1 page 223.

[35] V.A. Khoze, S. Lupia and W. Ochs, Phys. Lett. **B394** (1997) 179.

[36] C. Adloff *et al.* (H1 Collaboration), DESY preprint, DESY 97-164 (1997), submitted to Zeit. Phys.

[37] M. Glück, E. Reya and A. Vogt, Phys. Rev. **D46** (1992) 1973.

[38] M. Glück, E. Reya and A. Vogt, Zeit. Phys. **C53** (1992) 127.

[39] V.A. Khoze, S. Lupia and W. Ochs, hep-ph/9711392.

[40] "*ep* Physics beyond 1999", H1 Collaboration, H1-10/97-531, available from the authors on request.

[41] I. Abt *et al.* (H1 Collaboration) Nucl. Instr. and Meth. **A368** (1997) 310;
Ibid. 386.

[42] G.A. Beck *et al.*, Nucl. Instr. and Meth. **A367** (1995) 386;
W. Pilgram, Ph. D. thesis, University of Aachen, 1993 (unpublished);
pre-print PITHA 93/22 IIIB Phys. Inst. TH-Aachen.

[43] S. Burke *et al.*, Nucl. Inst. and Meth. **A373** (1996) 227.

[44] C. Cormack, First year Ph. D. project report, University of Liverpool 1994 (unpublished).

[45] CERN Program Library Q123.

[46] S. Eichenberger *et al.*, Nucl. Inst. and Meth. **A323** (1992) 532.

[47] M. Cuje *et al.*, DESY preprint, DESY-PRC-98/02 (1998).

[48] R. Bacher *et al.*, "HERA Luminosity Upgrade", draft of 30/3/98.

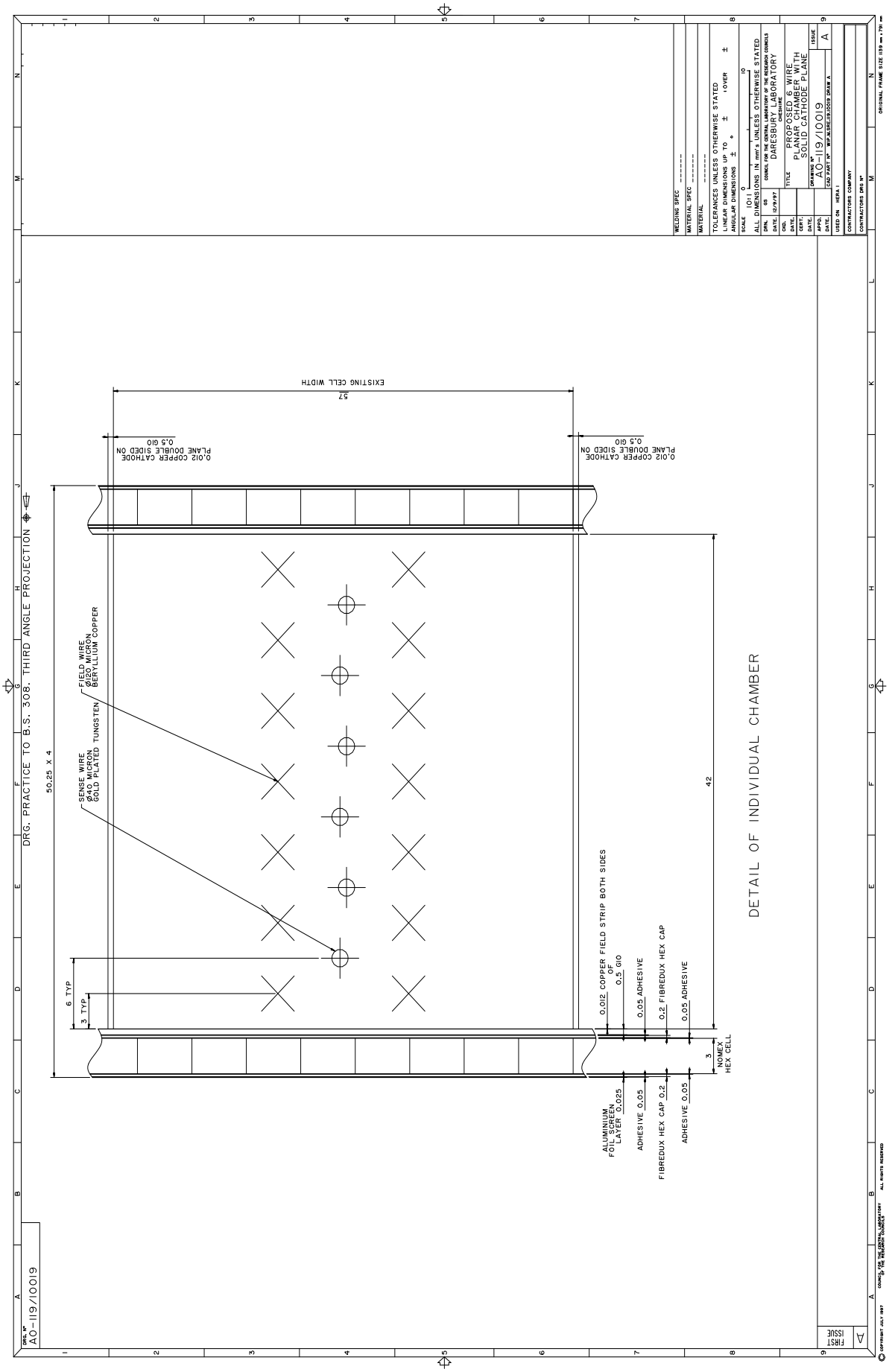

Figure 11: A section through one of the cells of the proposed new planar chambers.

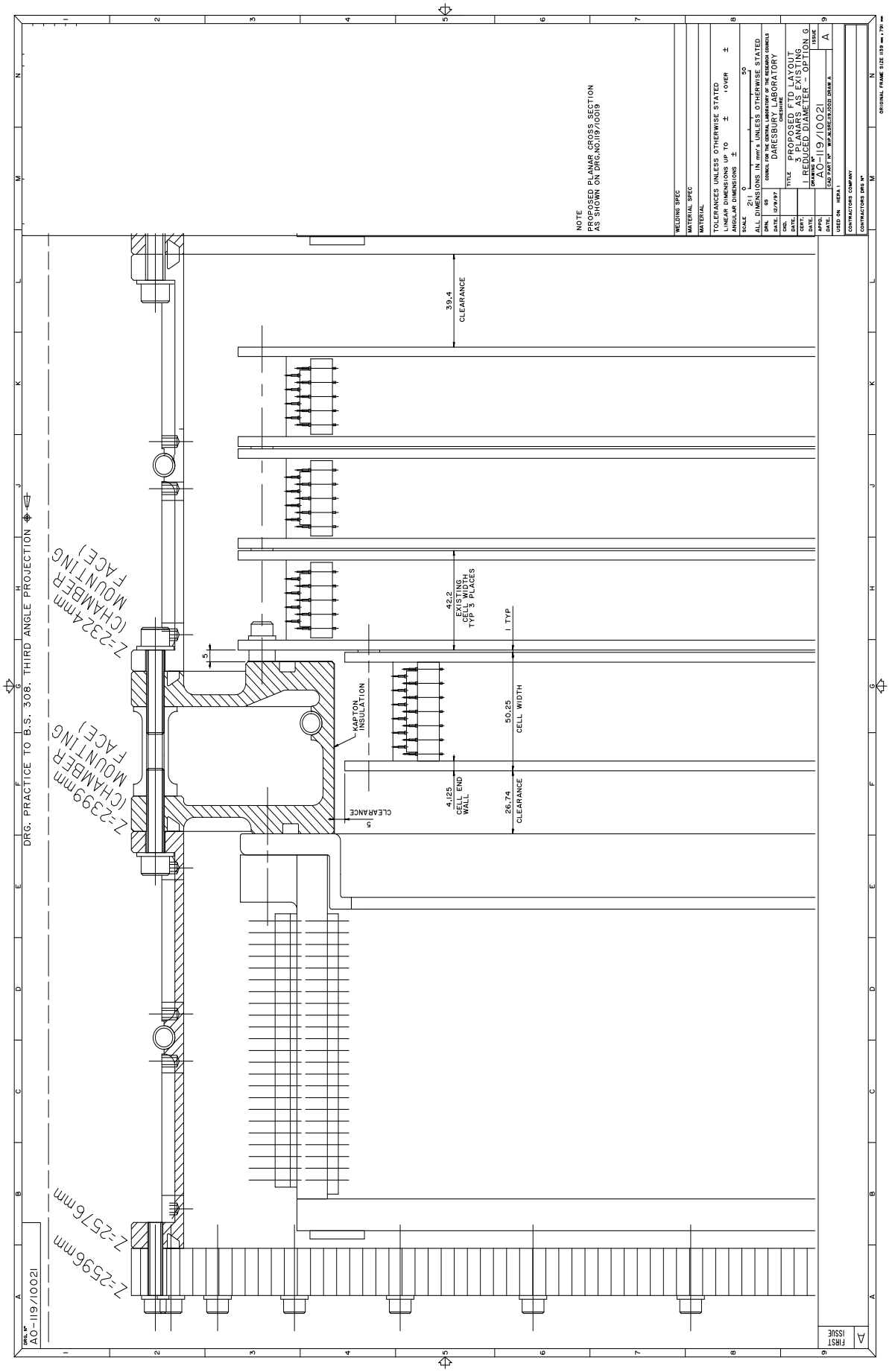

Figure 12: A section of an upgraded planar module, showing one of the new planar chambers (centre) in the position currently occupied by the transition radiators and the MWPCs, to the left of the new planar is a radial chamber and to the right three planar chambers from the current FTD.

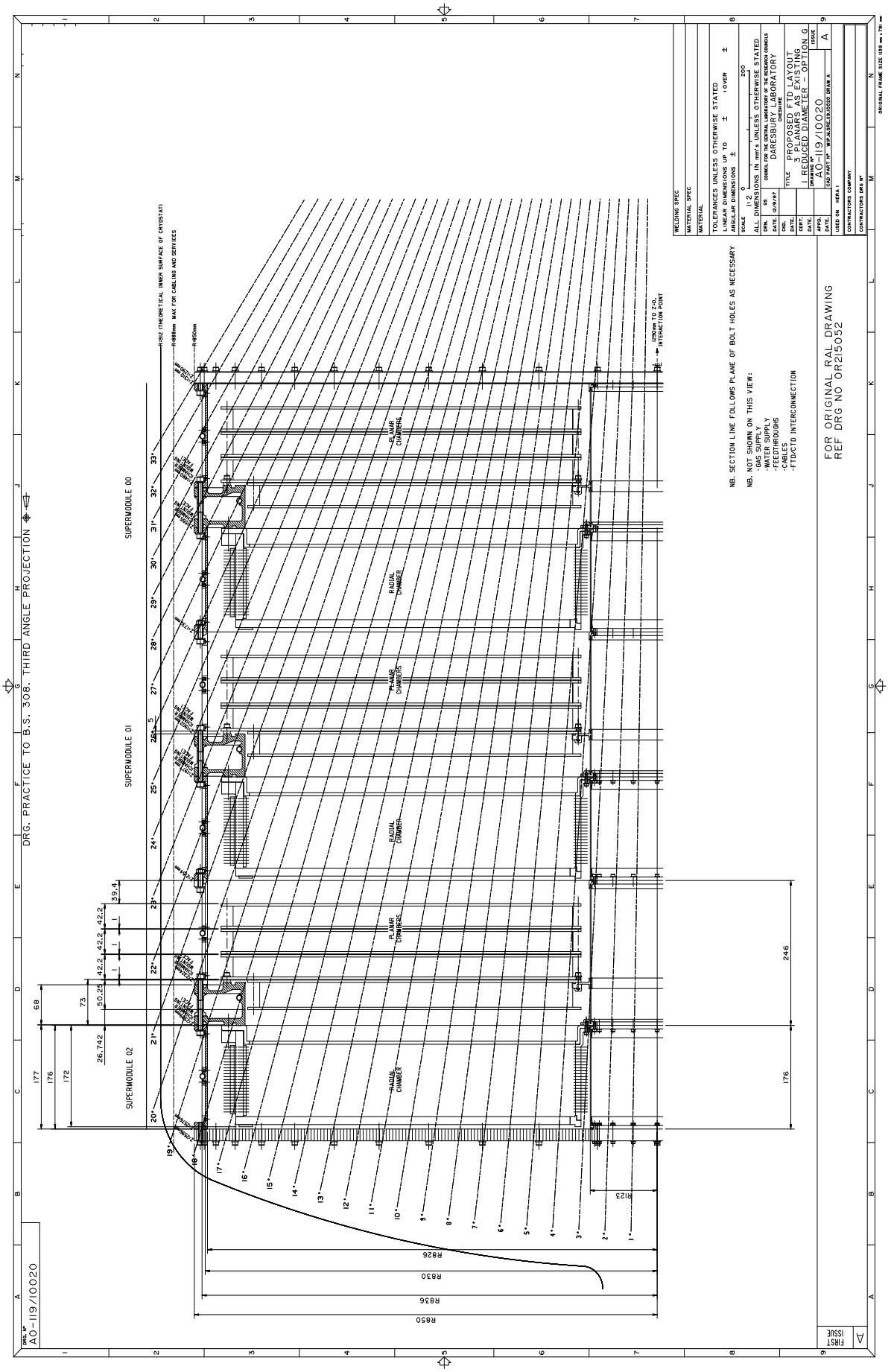

Figure 13: The proposed forward track detector with the three new planar chambers sandwiched between the radial and planar chambers of the current FTD.

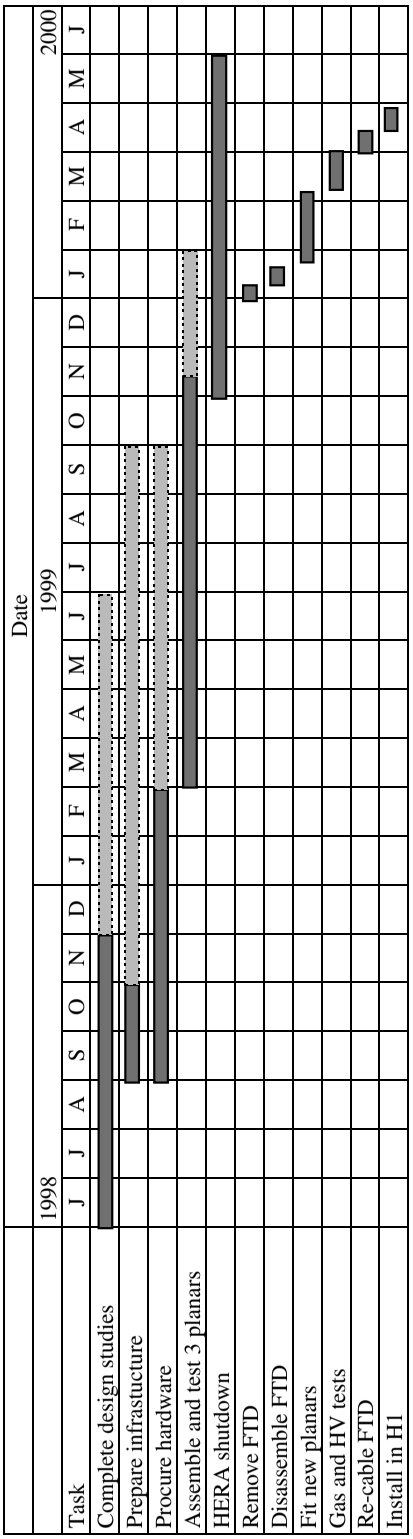

Figure 14: Schedule of work for the FTD upgrade, *i.e.* construction and testing of three new planar chambers at Daresbury, dismantling of the FTD at DESY, re-assembly incorporating the new planar chambers.

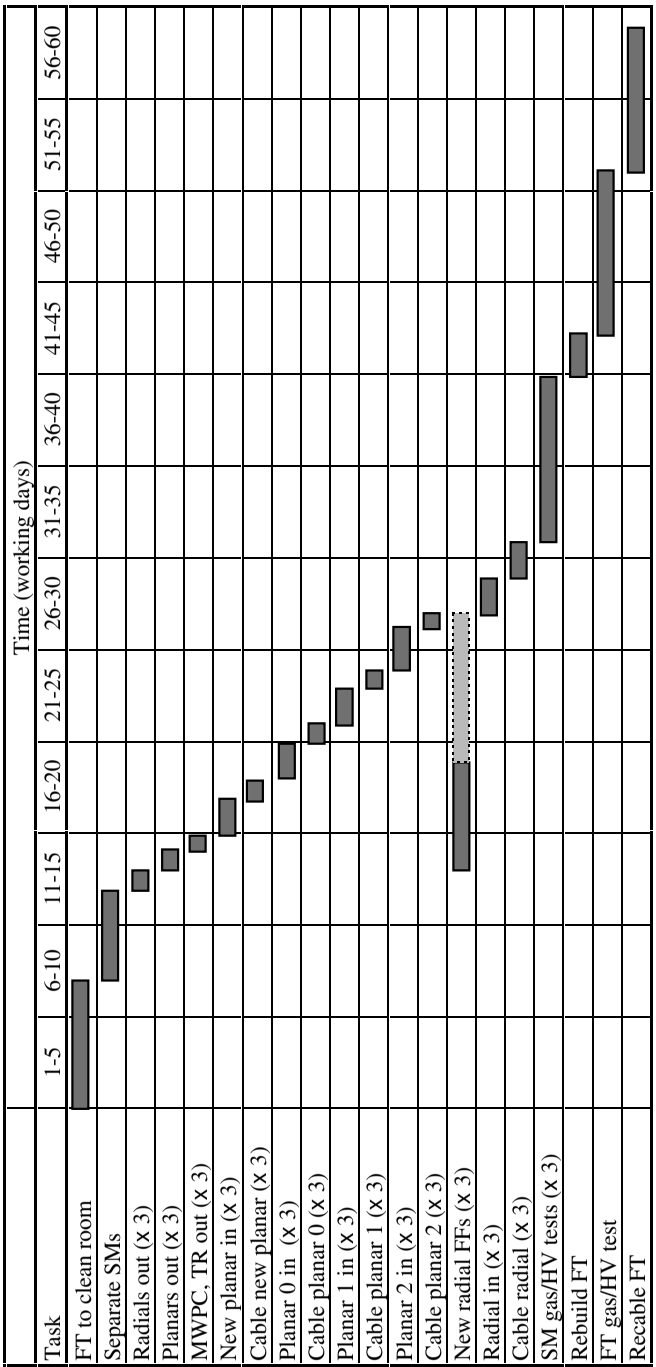

Figure 15: Preliminary chedule of FTD upgrade work to take place at DESY.